Investigating and Testing the Application of High-Performance Structural Adhesives for a Novel Aluminium Monocoque Formula Student Chassis and Suspension

A. Delgado, C. Mortiboys, M. Hoogeveen, M. Watkins, U. Singh.

1.0 Abstract

The aim of this report was to investigate the use of structural adhesives for the build of a novel aluminium monocoque chassis structure, and carbon fibre suspension members to provide a lightweight body structure solution. Firstly, the reliability and repeatability of two adhesives were tested, with a targeted error margin of ±10 %. Although Sika Power provided an improved performance compared to Kisling 7490 of 460 % with T-Peel and a 142 % performance increase in lap Shear Testing, the error ranges were significantly above 10 %, so demand greater testing if developed to the full manufacturing stage. Furthermore, it was found that the novel chassis structures could be accurately simulated via finite element analyses as verified through a physically tested partial chassis model. Using validated CAE models, the full chassis is predicted to have a torsional rigidity of 2 429 Nm/deg with a torsional efficiency of 71.4 Nm/deg kg compared to 61.7 Nm/deg kg for a steel tubular equivalent. For the suspension members it was found that knurling improves the performance of the composite-metal joints by 43.6 % and 18.3 % for longer and shorter inserts, respectively, but increased the variability to values greater than ±10 %. Overall, this study shows that vehicle mass can be reduced by 17 kg by utilising structural adhesives in a novel chassis structure.

2.0 Introduction

The use of adhesives within the automotive sector has seen increasing popularity due to the ability to reduce joint mass compared to mechanical fastening. As such, this report aims to investigate the use of structural adhesives for the manufacture of an aluminium monocoque chassis structure and suspension system for the next generation Warwick Racing Electric Vehicle (WRe3) for the Formula Student UK (FSUK) competition. Firstly, adhesive strength and preparation is investigated via coupon testing using lap-shear and T-peel tests. Following this a 3-piece extruded aluminium beam is bonded and tested with its results being compared to that of a Finite Element Analysis (FEA). Furthermore, a chassis subsection, namely the driver's compartment, is designed, built, physically tested, and compared to FEA results. The application of adhesives for the use of suspension member construction is also studied. The composite-metal joints are pull-tested and the effect of knurling patterns on the performance of the bond is investigated. An insert with no knurling is used as a base case for comparison and 3 different knurling patterns are created by varying the depth of the knurl and the length of the insert.

3.0 Adhesive Coupon Testing

3.1 Coupons and Adhesive Selection

ISO 4587 [1] is used to identify the Tensile Lap Shear Strength of an adhesively bonded surface and this serves as a suitable comparator between adhesives. ISO 11339 [2] is a test that identifies the tensile peeling strength of the adhesive. To establish a benchmark for testing, the technical data sheet values of Sika Power 880 were assessed and demonstrate that a Lap-Shear strength of 23 MPa should be achievable using the desired surface treatment mechanisms [3]. Two adhesives with data sheet properties that exceed those of Sika Power 880 were tested to demonstrate a repeatable exercise of surface treatment, curing and adhesion properties using the ISO tests stated.

Adhesive	*Chemical Base*	*Curing Time (23ºC)*	*Curing Time (85ºC)*	*Lap Shear Strength (MPa)*	*Tensile Strength (MPa)*
Sika Power 880 [3]	2-component (epoxy-amine)	7 days	4 hours	23	22
Sika Power 447-R [4]	2-component (epoxy-amine)	7 days	4 hours	28	28
Kisling 7490 [5]	2-component (epoxy-hardener)	15 hours	65 minutes	33	34

Table 1: *Comparison of selected adhesives for testing*

3.2 Surface Treatment

Previously, the standard discipline within industry-led research at Warwick Manufacturing Group (WMG) was manual abrasion using a Scotch-Brite Aluminum Oxide Abrasion Pad with a cleaning stage both before and after abrasion using acetone. Collaborative study between WMG and Ford Manufacturing found this has been acceptable at producing a repeatable data set. In addition, the University houses a shot blasting station for surface abrasion, but the dimensions available are inadequate for the chassis subsection and for the larger chassis that will eventually be produced as the project develops from a concept to a development model. This makes it unsuitable as a surface treatment option. Therefore, this study utilises manual abrasion techniques to remain within the scope of the study.

3.3 Curing

The standard discipline for curing is to utilise both room temperature curing and the Rolls-Royce Curing oven (volume of one cubic metre) within the Materials Characterization Laboratory to accelerate coupon development. From this, temperature can be monitored and controlled to a desired temperature of 85 ºC, as seen in Table 1. The dimensions of the oven also allow the chassis subsection to be cured at a higher heat, allowing for greater coherence between the chassis subsection and the coupon performance. As a result, both coupons and the chassis subsection underwent standard room temperature curing for 5 days and accelerated oven curing at 85 ºC for one hour. Throughout this, bonded surfaces and elements were clamped using their respective methods.

3.4 Results

3.4.1 Lap Shear

Figure 1 shows the mean Lap Shear Strength of both Sika Power 447-R and Kisling 7490, also showing the standard deviation of each adhesive via an error bar. It is evident that Sika Power 447-R produced an improvement over Kisling 7490, with a mean increase of approximately 5.0 MPa and improvement to the coefficient of variance from 51 % to 12 %. Sika Power Lap Shear testing therefore lies close to the targeted coefficient of variance desired from this testing. Failure of both adhesives was identified as adhesive failure, as fracture showed adhesive had not successfully bonded to the substrate equally on both sides.

3.4.2 T-Peel

Figure 2 shows the mean T-Peel Strength of both Sika Power 447-R and Kisling 7490, again showing the standard deviation of each adhesive via an error bar. There is a substantial improvement to the mean of the maximal load increase of 460 %. However, there is a much larger coefficient of variance for both adhesives compared to that of Lap Shear, with Sika Power 477-R having a coefficient of variance of 33 %, and Kisling 7490 with 103 %. This does not lie close to the desired coefficient of variance and leads to poor confidence in the achieved results. This test also demonstrated clear adhesive failure, with little to no adhesive present on one side of the T-Peel sample.

3.5 Analysis

From the results seen in Figure 1 and 2 as well as the coefficients of variance stated, Sika Power yields a performance increase of 146 % with regards to Lap Shear Strength and a 460 % performance increase to that of Kisling 7490 with regards to T-Peel. However, all coefficients of variance were above the desired 10 % value, showing that further testing outside the scope of the project is required. If the project is to progress further to a full manufacture and competition stage of development, it is required to continue coupon testing with various adhesives until a 10 % coefficient of variance is achieved. In addition, there is consistent adhesive failure of joints. Therefore, surface treatment could be investigated also for increases

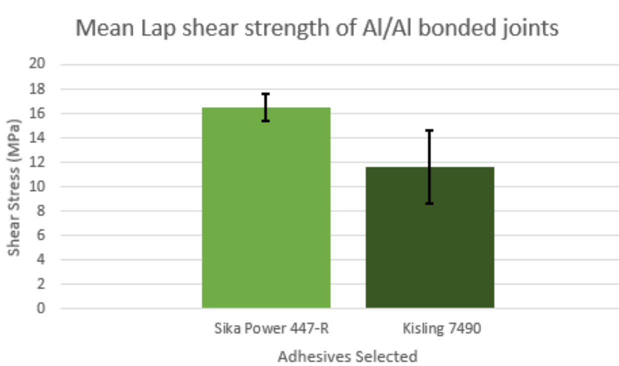

Figure 2: *Mean Lap Shear Strength of Aluminium-to-Aluminium Bonded Joints*

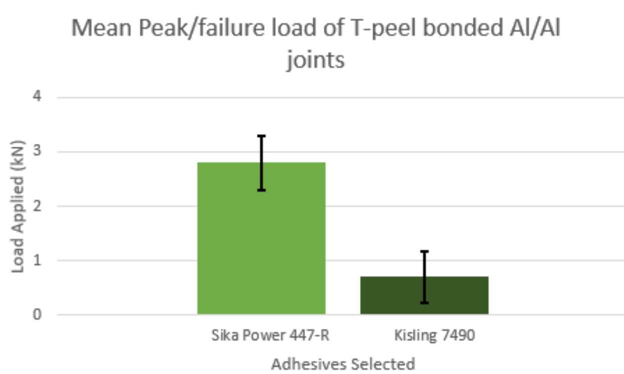

Figure 2: *Mean Peak/Failure Load of T-Peel Bonded Aluminium-to-Aluminium Joints*

in performance in techniques such as shot blasting can be deemed viable for a larger structure. However, there is no overlapping of standard deviations shown by error bars, determining that across all coupon testing, Sika Power exhibits improved performance. This made it viable as an adhesive for chassis subsection manufacture.

4.0 Body Structure Simulation and Testing

As part of the testing and verification plan, a representative test section of the novel chassis was made within which the driver sits. The test section was adhesive bonded using Sika 477-R and consists of four extruded aluminium beams, two bulkheads at each end, three honeycomb aluminium panels and eight fixtures connecting the beams and bulkheads, seen in Figure 3. A fundamental technique for benchmarking a chassis is via its torsional rigidity and impact resistance. As such, these factors were investigated via physical testing and FEA simulations to compare results and were used to predict full chassis benchmark factors.

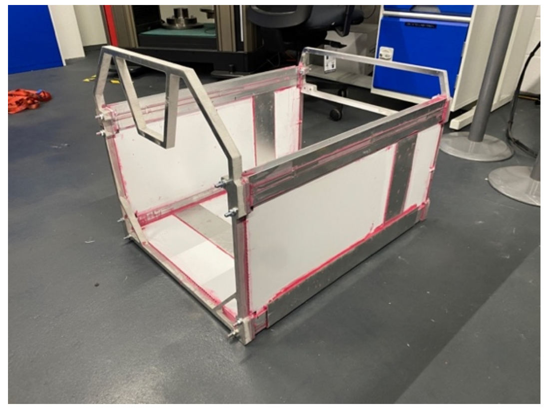

Figure 3: *Chassis Test Section*

4.1 Extruded Beam Testing

A physical 3-point bend test of an extruded aluminium beam was completed to help validate the strength and impact resistance of these members for use in the chassis. This test helped to emulate a similar load case for the side intrusion test. Comparing the deformation of the extruded beam after an 8 kN static load case for a 3-point bend test from FEA analysis to the physical test done on the Instron 5985, it was found that the physical test performed better than the FEA simulation. By measuring the deflection against the

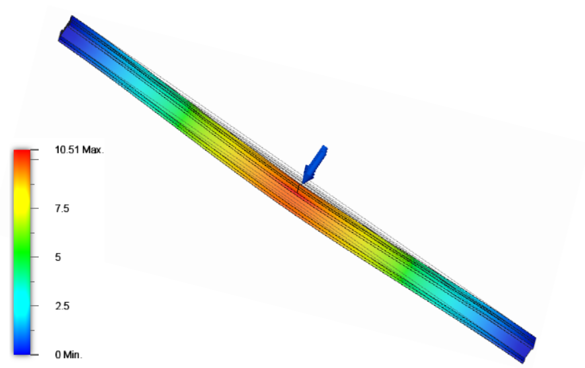

Figure 4: *FEA Simulation of 3-Point Bend Test*

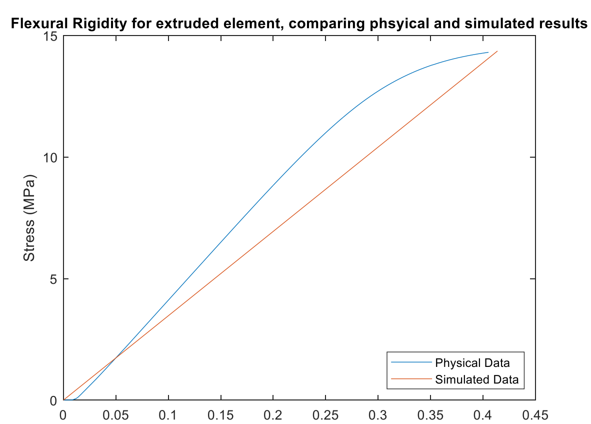

Figure 5: *Comparison of Physical Data to Simulation Data of 3-Point Bend Test*

input load for both the physical model and the simulation, the physical model was seen to perform better than the simulation as seen by the higher flexural stiffness in Figure 5, showing higher stresses. This was due to the adhesive adding thickness to the extrusion which inherently increased the second moment of area, thus increasing the flexural rigidity of the beam as well as the multiple components compounding more strength on the individual components within the beam. This validates the use of the adhesive and the design of the extruded aluminium beam.

4.2 Chassis Section Testing

For the physical chassis section test, a 75kg mass was placed 1 metre from the longitudinal centre on a steel rod to generate a torque of 735 Nm at the bottom corners on the front bulkhead with the rear bulkhead fixed. This resulted in 9.8 mm of deflection as measured by a Dial Test Indicator (DTI) located under the left-hand side of the front bulkhead. An FEA simulation was set up in similar fashion, applying the same torque as the lower front section of the bulkhead and constraining the bottom surface of the rear bulkhead. The results of this simulation, seen in Figure 6, showed that there was little deflection towards the rear of the test box, with most of the rear having a displacement less than 4 mm. It was noted that the deflection across the test box was almost symmetrical, with a skew for more displacement on the left-hand side of the section, where the torque was acting as a compressive force due to the fixed underside of the rear bulkhead.

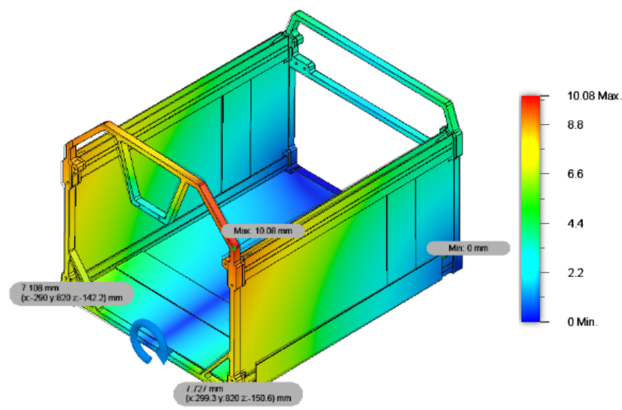

Figure 6: *Simulation Model of the Chassis Subsection under Torsional Load*

Comparing the physical test of the chassis section to the FEA simulations at the same torques applied, it was found that the physical testing provided a lower torsional rigidity (367 Nm/deg) compared to the simulated test section (525 Nm/deg). The physical test produced a value that was 30 % lower than the simulated test box, the comparative torsional stiffness is shown in Figure 7. A reason for this may be that the test section was not suitably fixed into place on the testing table or inaccurate measurement in the applied masses in the physical test.

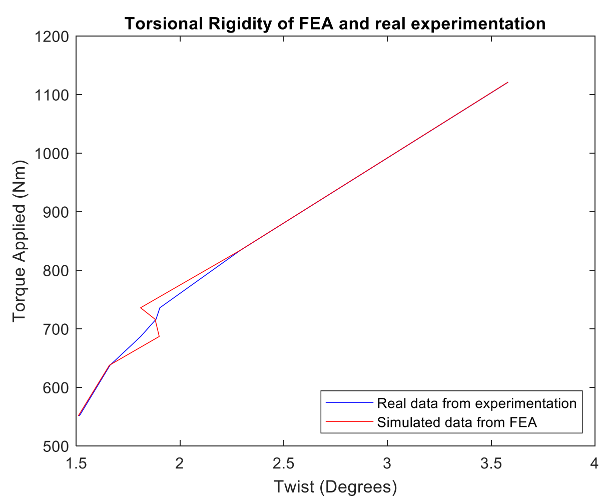

Figure 7: *Comparison of Physical Data to Simulation Data for Torsional Rigidity*

A full chassis FEA was then performed, using the validated input data and approach from the test section FEA to predict real-life performance. This simulation predicted a full body structure torsional rigidity of 3470 Nm/deg. This value is reduced by 30 % as per the discrepancy between simulation and test results. This indicates a predicted torsion stiffness of 2 429 Nm/deg. Steel tubular equivalent chassis structures commonly have a torsional stiffness between 1 800 Nm/deg [6] and 2 100 Nm/deg [7], demonstrating that this novel chassis design performs strongly against tubular steel equivalents whilst reducing mass by up to 30 %.

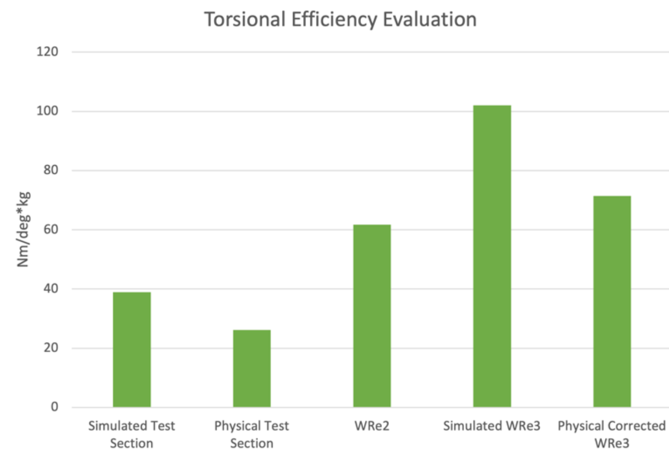

Figure 8: *Comparison of Physical Data to Simulation Data of Torsional Rigidity*

The overarching performance of the test section, WRe3 chassis and benchmarking WRe2 chassis were compared against each other by calculating the torsional efficiency using chassis mass. Comparing the results in Figure 8, it was observed that the test box had low torsional efficiency even with its significantly lower mass, which is likely a result of the test section being the widest section of the vehicle with the least support. The torsional stiffness of Wre2 was higher than the corrected WRe3 torsional rigidity, by 288 Nm/deg. However, with the masses taken into consideration whereby WRe3 has a lower mass by 10 kilograms compared with WRe2, the torsional efficiency of the corrected WRe3 chassis was greater than WRe2, being around 20 % more efficient.

5.0 Suspension Testing

The main aim of the design of the suspension was light weighting the system while keeping or improving its performance over its predecessor [8]. To do this, Carbon Fibre (CF) tubes were investigated as a viable suspension alternative, utilising threaded inserts that are bonded to the CF tubes using a purpose-specific adhesive.

5.1 Testing and Subject Structure

Research suggests that knurling patterns can increase the strength of metal-composite bonds through mechanical interlocking [9, 10]. Following this, 4 separate patterns for knurling were designed, with two inserts with no knurling used as reference values for a Pull-Out test. The test would determine if the bonded surface and the adhesive would be strong enough to resist the worst-case loads. The tests were repeated 3 times for each design, to ensure results were accurate and to mitigate the variation generated surface preparation discrepancies and machining tolerances. Additionally, all inserts were machined by the authors from Aluminium 7075 and were turned down to have an Outer Diameter (OD) of 17.4 mm ± 0.1 mm, an M8 thread on the inside and bonded to a 100 mm Roll Wrapped tube with a 20 mm OD.

For this study, the adhesive selected was Kisling 1665 for its versatility with a wide range of composites, quick curing time and adhesive characteristics [11]. Additionally, the adhesive was supplied as sponsorship, which was an important consideration due to limited project funding. The surface preparation was kept constant as this would add an additional unwanted variable. All inserts were media blasted using Aluminium Oxide to create surface abrasion and improve the performance of the bonds and repeatability of the data [12]. However, the CF tubes were manually abraded as the fibres could be damaged when exposed to a media blasting machine and was done using a 7448 ULF hand pad from 3M. The cleaning stage for both materials was kept consistent with coupon testing due to its simplicity and effectiveness. The adhesive reaches its final strength after a curing time of 12 hours at 23 ˚C [11] which led to the metal-composite joints were left to cure for > 72 hours at 23 ˚C to ensure they reached their full strength.

The Pull-Out test was conducted on an Instron 30k machine and two 65mm High-Tensile Steel studded M8 rod were used to enable gripping in the v-grooved jaw face: this exerts a tensile force on the inserts. This also emulated the effect a threaded rose joint would have on the metal-composite joint. The rod was clamped on both ends and the test consisted of pulling the threaded bar at 2 mm/minute till the system experienced an extension of 10 mm.

5.2 Results

For these preliminary tests, a coefficient of variance under 10% would provide enough confidence to validate the use of adhesives in the full build of the vehicle. The mean peak values from the tests are presented in Figure 9 along with an error bar showing the standard deviation. The graph displays the data without the outliers. The reference data exhibited a mean peak load of 7.5 kN ± 0.25 with a variance of 3.3 %. However, it showed two adhesive failures, not bonding with the composite and incomplete curing, despite following the curing schedule.

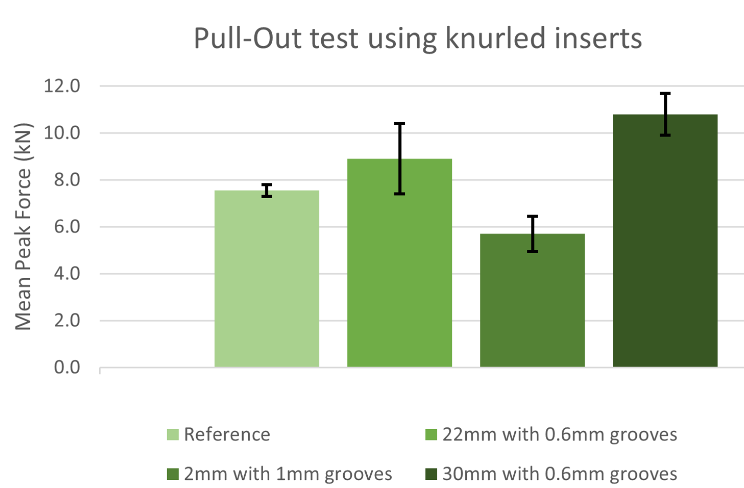

Figure 9: *Mean Peak Loads of Specimens with Different Knurling Patterns for a Pull-Out Test.*

The results for the smaller length inserts with shallower grooves are highly variable for extension at failure and peak load. Specimen 2 exhibited an incomplete cure, due to the texture of the adhesive bond in areas remaining sticky to the touch. Although following recommend curing procedures as stated from [11], the bond may have been improved with a thermal treatment stage as well. Figure 10 shows the failure on the insert of the specimen where the smooth region revealed almost the entire bonding area where there was no bonding with the CF tube. This is a consequence of improper surface treatment, where the tube was only sufficiently abrased near the end of the tube. The mean peak load for this design was calculated to be 8.9 kN ± 1.5 and had a coefficient of variance of 16.9 %. The design demonstrated improved performance but introduced inconsistency, leading to poor confidence in the data.

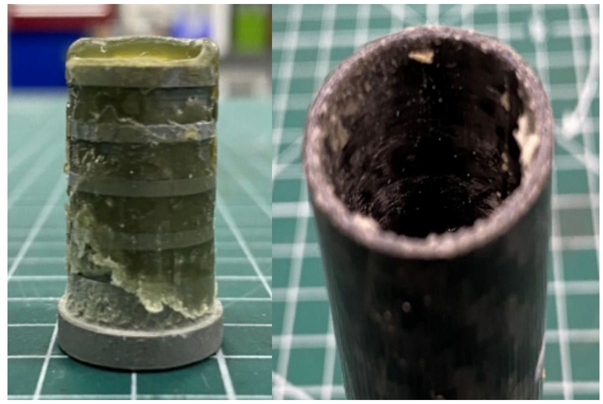

Figure 10: *Specimen 2 Insert (left) and Tube (right) Showing Adhesive Failure.*

The design with deeper grooves performed worse than the previous design because the large grooves reduced the bond area. A significant amount of bond strength was lost, and Figure 11 (top) shows that all three inserts underwent adhesive failure, evidenced by their smooth fractures. These inserts were only able to withstand a mean peak force of 5.7 kN ± 0.7, 75% of the reference data, and had a coefficient of variance of 13.1 %. The design demonstrated excessive knurling reduced performance of the joint and led to adhesive failure.

Lastly, the longer inserts performed the best of all the designs. Nevertheless, there was an outlier with this design that had a peak load of only 61.6 % of the mean of the other two specimens. Figure 11 (bottom right) shows the bonding failure of the specimen, and it is evident that the surface abrasion was inadequate and there was incomplete joint coverage where the base material was exposed between the grooves. The bonding for best performing specimen is shown on the bottom left of the same figure and the adhesive undergoes cohesive failure instead of adhesive failure. The mean peak load for this design was 11.8 kN ± 8.3, significantly higher than the reference data without knurling. It also had a lower coefficient of variance, 8.3 %, than the previous two designs.

Figure 11: *Specimen Inserts 4 - 6 from Left to Right on Top and 7 and 9 Bottom Left and Right, Respectively*

Indicative tests found that knurling improved the performance of the composite-metal joint, but only for shallower grooves, by 43.6 % and 18.3 % for the longer and shorter inserts respectively. Additionally, the best performing design was the 30mm insert which provided the greatest bond area and therefore the maximum amount of adhesive. However, it was also observed that incorrect surface treatment led to poor results, regardless of the knurling pattern design. As such, it is imperative to have a standard surface treatment procedure to mitigate the high variation in the composite-metal joints. Furthermore, of the knurled inserts, only the final design provided sufficient confidence with a coefficient of variance of 8.3 %. Supplementary tests need to be conducted to investigate the ideal choice of adherends and adhesives and gain greater confidence in the results before bonded CF tubes can be used for a full build chassis. Additionally, the use of an oven post-cure can be examined to ensure optimum performance of the joints.

7.0 Suggestions for Further Improvement

With regards to adhesive testing, there is a large variance in collected data for all adhesives, in particular for Kisling 7490. This is due to the adhesive not performing initially as anticipated from technical datasheets and requiring increased testing. This began to threaten the project output as continuing to test adhesives until variance was reduced and the desired lap shear strength was achieved may have prolonged further manufacture, limiting the physical output from this project. Therefore, to ensure future improvement, adhesives and coupon testing must be progressed to encompass more adhesives and, in general, more tests. Doing so will produce richer information that will serve well in validating manufacture to the competition scrutineers and allow for increased confidence in the performance of the chassis.

With regards to the pull-out tests conducted for the carbon fibre reinforced composite rods, there is a need to continue adhesive selection and optimisation. Multiple issues arose regarding performance and curing, which can be studied further outside the project scope. From this study, it is evident that the potential for pull-out rods exists, and the confidence can be increased via inserts with knurling patterns and a lesser penetration depth. In a similar manner to coupon testing, more adhesives can be tested which will improve the quality of the product.

In summary, the improvement of the study harbours around adhesive testing and variance. With the use of a non-homogeneous material leading to difficulties with simulation, justification of any model is difficult without a coherent and repeatable adhesive joint present. Impacting both the chassis and the suspension, increased testing and a larger testing window may aid in developing increased trust in the model and the performance of the adhesive. However, the purpose of this study is to serve as the foundation towards developing a novel aluminium monocoque chassis structure with lightweight carbon fibre suspension system. Therefore, this should be targeted first if the WRe3 is to be produced for future competition.

7.0 Conclusion

In conclusion, a fully aluminium bonded chassis has been developed, with the testing of a subsection shown via both FEA and a physical model to allow for validation. This was done by first assessing adhesive selection and progressing the utilisation of said adhesive to produce a chassis with both the extruded elements and the section produced within the scope of the project. With a difference of 2.81 % in flexural rigidity from simulation and physical testing of the aluminium extruded beam, the FEA simulation validates the novel monocoque full body structure design. The torsional stiffness of the WRe3 chassis is predicted to be 2 429 Nm/deg which is higher than a standard steel tubular chassis. The WRe3 chassis had a calculated torsional efficiency of 71.4 Nm/deg kg which is 15.7 % more efficient than the previous generation chassis whilst being lighter and easier to build. In addition, the feasibility of using CF tubes and threaded inserts for wishbone suspension modelling was investigated, with another adhesive. Various knurling patterns were tested and revealed a 43.6 % improvement in performance for the best design. This demonstrated the weight saving potential provided by the adhesives in enabling the use of CF tubes within the suspension system.

8.0 References

[1] British Standard, “Adhesives – Determination of tensile lap-shear strength of rigid-to-rigid bonded assemblies”, BS ISO 4587:2003, (Accessed: March 6, 2023).

[2] British Standard, “Adhesives – T-peel test for flexible-to-flexible bonded assemblies”, BS EN ISO 11339:2010, (Accessed: March 6, 2023)

[3] SikaPower (2022) SikaPower 880 2-component Structural Adhesive Product Data Sheet, SikaPower. Available at: https://industry.sika.com/content/dam/dms/gb01/t/sikapower-880.pdf (Accessed: February 28, 2023).

[4] SikaPower (2017) SikaPower 477-R Structural and Crash Resistant 2 Component Adhesive Product Data Sheet, SikaPower, (Accessed: March 8, 2023).

[5] Kisling, K. (2023) Technical DATASHEET 7490 - kisling, Kisling 7490 Technical Data Sheet. Available at: https://www.kisling.com/fileadmin/dateiliste/dokumente/Technische_Datenblaetter/EN/TIS_7490_e.pdf (Accessed: March 8, 2023).

[6] Costa, J.A. and Vilela, D. (2014) “Formula SAE frame torsional stiffness study using FEA,” SAE Technical Paper Series[Preprint]. Available at: https://doi.org/10.4271/2014-36-0234.

[7] Ary, A.K. et al. (2021) “Numerical estimation of the torsional stiffness characteristics on urban shell Eco-Marathon (SEM) vehicle design,” Curved and Layered Structures, 8(1), pp. 167–180. Available at: https://doi.org/10.1515/cls-2021-0016.

[8] Singh, U. et al. (2023) Warwick Racing: Body Structure and Chassis Dynamics. rep. Coventry, Warwickshire: School of Engineering.

[9] Esfandiari mazandaran, S., Shakouri, E. and Haghighi, S.E. (2020) “The effect of knurling surface treatment on the strength of adhesively bonding between steel plate and carbon-phenolic composite,” Iranian Journal of Manufacturing Engineering, 7(5), pp. 44–55.

[10] da Silva, L.F.M. et al. (2010) “Effect of grooves on the strength of adhesively bonded joints,” Adhesion & Adhesives, 30(8), pp. 735–743. Available at: https://doi.org/https://doi.org/10.1016/j.ijadhadh.2010.07.005.

[11] Kisling (2022) Technical DATASHEET 1665 - kisling, Kisling. Available at: https://www.kisling.com/fileadmin/dateiliste/dokumente/Technische_Datenblaetter/EN/TIS_1665_e.pdf (Accessed: March 7, 2023).

[12] Rudawska, A. et al. (2016) “The effect of sandblasting on surface properties for adhesion,” Adhesion & Adhesives, 70, pp. 176–190. Available at: https://doi.org/https://doi.org/10.1016/j.ijadhadh/2016.06.010.